Electronic Supplementary Material (ESI) for Analytical Methods.

Silicon Nanoparticles: Fluorescent, Colorimetric and Gel Membrane Multiple Detection of Cu^{2+} and Mn^{2+} as well Rapid Visualization of Latent Fingerprints

Baoya Zhu,[a] Mingyu Tang,[a] Liying Yu,[a] Yaoyao Qu,[a] Fang Chai,[ab*] Lihua Chen[b*] and Hongbo Wu[a*]

[a.]Key Laboratory of Photochemical Biomaterials and Energy Storage Materials, Colleges of Heilongjiang Province, College of Chemistry and Chemical Engineering, Harbin Normal University, Harbin 150025, P. R. China. E-mail: fangchai@gmail.com

[b] Shandong Key Laboratory of Biochemical Analysis; College of Chemistry and Molecular Engineering, Qingdao University of Science and Technology, Qingdao 266042, PR China.

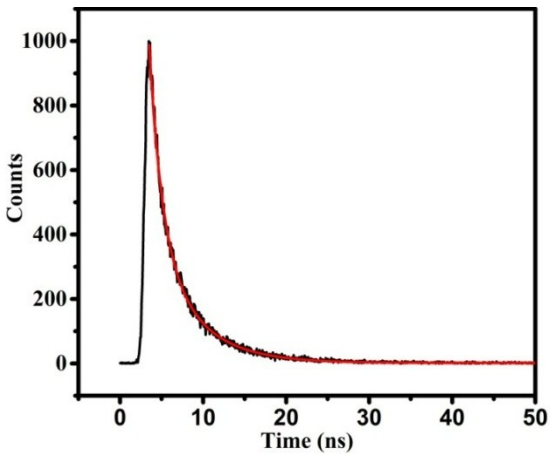

Figure S1 The fluorescence decay curves for Si NPs.

To investigate the practicability of Si NPs towards the determination of Cu^{2+} in real samples, tests were determined under the optimum conditions. As shown in Figure S1 A, the intensity of fluorescence emission was enhanced at 425 nm with the increasing of Cu^{2+} concentrations. As the concentration of Cu^{2+} increased, the fluorescence intensity of Si NPs enhanced significantly (inset Figure S1 A). Figure S1 B expresses the linear relation-ship of I/I_0 values versus the Cu^{2+} concentrations in the range of 1-10 μM with the correlation coefficient R^2=0.99045. The limit of detection was estimated to be 0.72 μM. These results confirmed that the sensor system based on Si NPs displayed satisfactory sensitivity towards Cu^{2+} at low concentrations.

The reliability of the as-prepared Si NPs in practical application was evaluated by Cu^{2+} detection in environmental sample. Upon increasing the concentration of Cu^{2+} in the solution in the range of 0-20 μM, a significant enhancement of absorbance peak at 425 nm was obtained as the solution turned from colorless to pale yellow (Figure S1 C). As shown in Figure S1 D, a linear relation curve was obtained by recording the relationship between the ratios of A/A_0. The detection limit was found to be 1.09 μM. Besides, as the concentration of Cu^{2+} increased, the color of the solution turned to pale yellow, which could be discriminated distinctly (Figure S1 E). These results illustrate that the detection of Cu^{2+} can be performed by this colorimetric methodology, which permitted the monitoring

of Cu^{2+} on site and at any time.

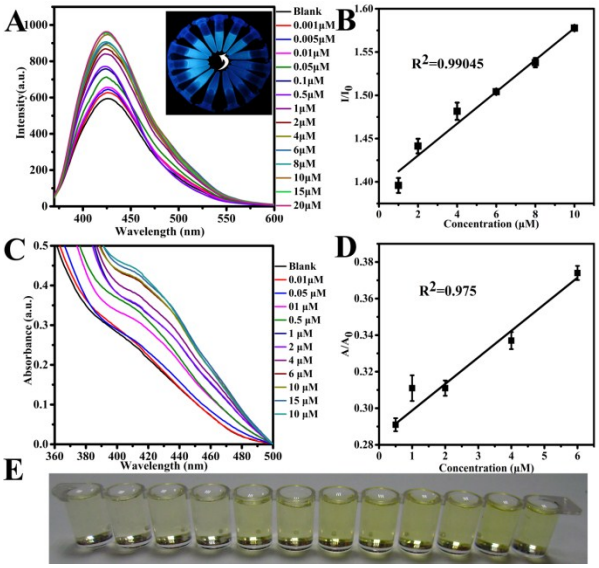

Figure S2 (A) The fluorescence spectra (λ ex=345 nm) of Si NPs upon the addition of different concentrations of Cu^{2+} ion in real sample, the inset image corresponds to the photo taken under the UV lamp. (B) The dependence of fluorescence intensity ratio values (I/I_0) on the concentrations of Cu^{2+} in real sample. (C) UV-vis spectra of Si NPs upon the addition of different concentrations of Cu^{2+} ion in real sample. (D) The linear relation curve of absorbance ratio (A/A_0) of Si NPs upon the addition of different concentrations of Cu^{2+} ion in real sample. (E) Photograph of corresponding solutions.

Similarly, the detection of Mn^{2+} in real water samples was performed. Figure S2 A showed the fluorescence spectra of Si NPs with Mn^{2+} in lake water. Corresponding, the fluorescence intensity increased continuously with increasing the concentrations of Mn^{2+}, which can be noticed by the images (inset Figure S2 A). Upon gradual addition of Mn^{2+}, there was also a remarkable increase of fluorescence at peaked 425 nm. The linear values of I/I_0 was observed with increasing Mn^{2+} concentrations over the range of 1-10 μM with R^2=0.99817 (Figure S2 B). The limit of detection was estimated to be 0.65 μM.

Furthermore, the colorimetric recognition of Si NPs in lake water systems was completed to simulate the application of Si NPs toward the detection of Mn^{2+} in real environmental samples. As shown in Figure S2 C and Figure S2 E, similar colorimetric response occurred tough there is existed unknown contamination. There was a good linear relationship between the values of A/A_0 against the Mn^{2+} over the range from 0.005 to 20 μM (Figure

S2 D). The detection limitation for Mn^{2+} is about 0.65 μM. In conclusion, we have demonstrated a colorimetric sensor array that can simultaneously detect and identify Mn^{2+}. All these results manifested that the Si NPs can be treated as a fluorescent and colorimetric probe for sensing Cu^{2+} and Mn^{2+} with good sensitivity and selectivity, even in real water samples.

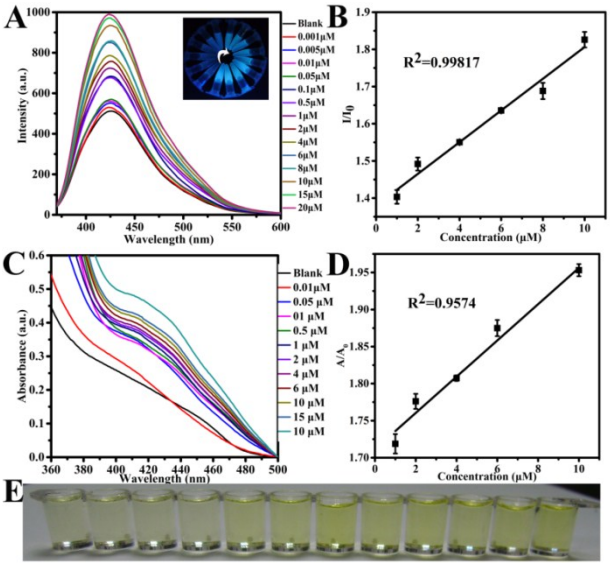

Figure S3. (A)The fluorescence spectra (λ ex=345 nm) of Si NPs upon the addition of different concentrations of Mn^{2+} ion in real sample, the inset image demonstrating changes in fluorescence. (B) The dependence of fluorescence intensity ratio values (I/I_0) on the concentrations of Mn^{2+} in real sample. (C) UV-vis spectra of Si NPs upon the addition of different concentrations of Mn^{2+} ion in real sample. (D) The linear relation curve of absorbance ratio (A/A_0) of Si NPs upon the addition of different concentrations of Mn^{2+} ion in real sample. (E) Photograph of corresponding solutions.

Table S1 Determination of element in Chagan lake water by ICP-AES

Element	**Mg**	**Cr**	**Mn**	**Fe**	**Ni**	**Cu**
Concentration (nM)	**15991.7**	**0.5**	**119.4**	**176.8**	**14.0**	**13.1**
Element	**Cd**	**Ba**	**Hg**	**Pb**	**Zn**	
Concentration (nM)	**0.9**	**20.9**	**0.1**	**1.1**	**78.1**	

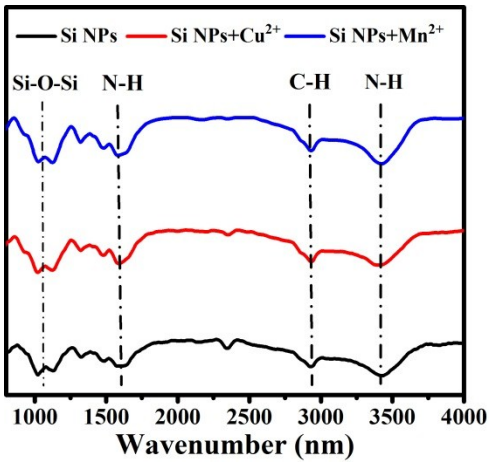

Figure S4. FTIR spectra of Si NPs, Si NPs+Cu^{2+} and Si NPs+Mn^{2+}.

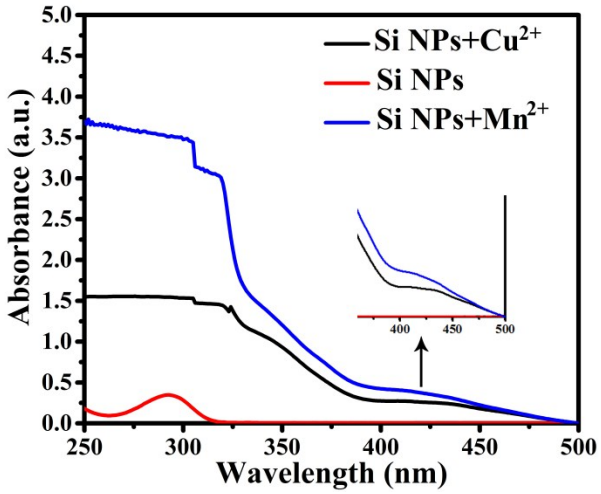

Figure S5. UV-vis absorption spectral of Si NPs and Si NPs upon addition of Cu^{2+} and Mn^{2+}.

HepG2 cells were cultured in Dulbecco's modified Eagle's medium with 10% FBS under 10% CO_2, 1% penicillin, and 1% streptomycin at 37℃ in a 5% CO_2/ 95% air incubator. Then HepG2 cells were grown on confocal dishes. Cells were washed three times with PBS buffer. Finally, the cells were imaged immediately using a confocal microscope.

The cell cytotoxicity of the probe was evaluated by MTT. The HepG2 cells were incubated with Si NPs of different concentrations (10, 20, 30, 40, 50 μM) for another 3 h. After incubation, the reagent was added to each well to assess the ATP activity.[1]

For biological application, the cytotoxicity of Si NPs was firstly evaluated through MTT assay by adding different concentrations of Si NPs in HepG2 cells (Figure S6). It can be seen that the cell viability was not decreased obviously after treating with 50 μM Si NPs for 3 h. The results indicated there was almost no cytotoxicity of Si NPs for long period incubation at low concentration. Therefore, it should be safe for bioimaging.[2] To further evaluate the potential application of Si NPs in living system, the imaging in living cell using Si NPs was investigated. The bright image of the HepG2 cells incubated with Si NPs indicated clearly the normal morphology of the cells, verifying that Si NPs was biocompatible and possessed minimum toxicity to the cells (Figure S6). As shown in Figure S7, it was obvious that HepG2 cells became quite bright owing to the strong fluorescence from Si NPs, indicating a large amount of Si NP had been internalized into the cells.[3] The images were obtained with green 174 channels (500-540 nm). These results indicated that the Si NPs can be applied in cell imaging due to their excellent biocompatibility and low cytotoxicity.[4]

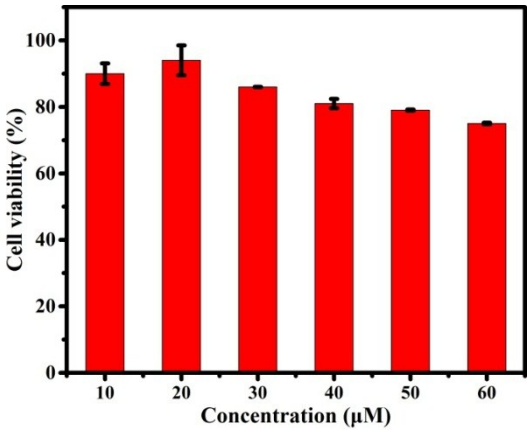

Figure S6. The viability of HepG2 cells after being incubated with Si NPs in the concentrations range from10 to 50 μM.

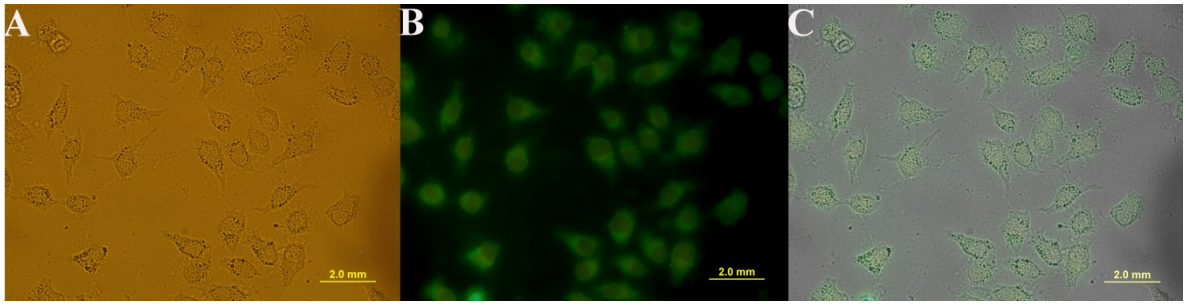

Figure S7. Confocal fluorescence images of live HepG2 cells. (A) Bright field image of the cells. (B) Fluorescence image of HepG2 cells after being treated with Si NPs. (C) Merged image of A and B.

1 P. C. Shen, Z. Y. Zhuang, Z. J. hao and B. Z. Tang, J. Mater. Chem. C, 2018, 6, 11835-11852.

2 L. Chen, G. C. Yang, P. Wu and C. X. Cai, Biosens. Bioelectron., 2017, 96, 294-299.

3 Y. Fang, W. Chen, W. Shi, H. Y. Li, M. Xian and H. M. Ma, Chem. Commun., 2017, 96, 8759-8762.

4 K. B. Li, F. Z. Chen, Q. H. Yin, S. Q. Zhang, S. Wei and D. M. Han, Sens. Actuators B: Chem., 2018, 254, 222-226.